3L-NPC AC-DC Power Converter Using Virtual Space Vector PWM with Optimal Switching Sequence Based on *g-h* Coordinate

Feng Guo, Tao Yang, Serhiy Bozhko, Patrick Wheeler
Power Electronics, Machine and Control Group (PEMC)
Department of Electrical and Electronics Engineering, University of Nottingham
Nottingham, United Kingdom
Feng.Guo@nottingham.ac.uk

***Abstract*—This paper presents a simplified virtual space vector PWM (VSVPWM) by using *g-h* coordinate for three-level neutral-point clamped power converter applications. The VSVPWM is a very appealing modulation technique due to the fact that the neutral-point (NP) voltage will be strictly balanced during one switching cycle. Current VSVPWM needs more calculation than the traditional SVPWM due to use more switching states. It can be seen that all virtual space vectors have special position in 60-degree frame. Therefore, sector/subsector judgment and dwell time calculation of VSVPWM can significantly avoid trigonometry functions (*sin/cos*) in *g-h* coordinate. This will significantly simplify calculation workload and thus allowing for being used in higher switching frequency application areas. In addition, the optimal switching sequence is selected to reduce even-order harmonics which has a bad impact on NP balancing issues in three-level power converter system. Finally, the correctness and effectiveness of VSVPWM based on *g-h* coordinate are verified through simulation results.**

***Index Terms*—3L-NPC AC-DC power converter, Virtual Space Vector PWM, *g-h* coordinate, Optimal switching sequence, Starter/Generator system, More-Electric-Aircraft**

I. Introduction

Since it was proposed by A. Nabae in 1981 [1], the three-level Neutral-Point-Clamped (NPC) converter shows great advantages over two-level converter. Compared with conventional two-level converters, three-level NPC converters shown in Fig.1 can achieve higher efficiency, lower EMI due to low *du/dt*, lower current total harmonic distortion (THD), and reduced voltage stress on individual components (as the voltage across the switches is only half of the DC-bus voltage instead of the full DC-link bus voltage in two-level AC-DC power converters). Recently, the three-level NPC converter has been widely used in high-capacity high-performance AC drives, renewable energy field, static VAR compensation systems, HVDC transmission system as well as electrical starter/generator systems in more-electric-aircraft (MEA) [2]–[6]. One of the major challenges of three-level converters is to balance NP voltage. This has been widely recognized by the researchers for many years. A large sum of methods have been proposed in past years [7]–[12]. The main solutions include using the redundancy of small vectors (P- and N-type small vector pairs) and utilizing a kind of feedback control technique. Dwell time can be redistributed with dynamic factor according to the voltage deviation between the upper and lower capacitors, so on and so forth. Nonetheless, the former cannot counterbalance the bad effect produced by medium-size vectors in higher modulation index, the latter is usually complicated to calculate accurate regulating factor in all conditions.

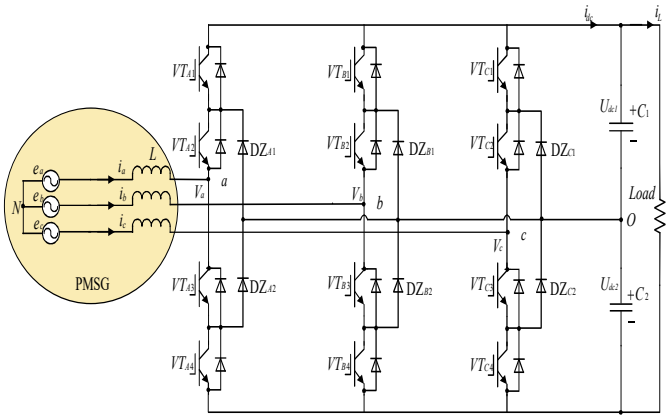

Fig. 1. Topology of 3L-NPC AC-DC power converter with PMSG.

In contrast, the authors in [13] came up with a novel thoughts based on a concept of virtual space vector PWM (VSVPWM). This method can essentially address the NP voltage imbalance issue. However, as mentioned by the authors themselves, these benefits are obtained at the expense of a higher output-voltage switching-frequency distortion [13]. Additionally, Switching sequence has a great influence on the AC waveform of the power converter as studied in [14], [15].

It has been reported that even-order harmonics negatively influence DC-link voltage balancing issues and can cause losses, overheating and other detrimental effects of generators [16]. More importantly, it has been proved that initial voltage drifts can be naturally balanced if only AC-side of three-level NPC power converter does not contain even-order harmonics with non-zero load resistance [17]. In order to eliminate even-order harmonics in the phase current, the switching sequence also should be optimally chosen in different sectors and

sub-sectors. In the meanwhile, dwell time calculation based on *g-h* coordinate can avoid using trigonometry functions (*sin/cos*), thereby achieving faster calculation time. A similar method with fast and simple SVPWM algorithm has been reported in [18]. Besides, it is crucial for achieving high switching frequency of power electronic devices especially for aerospace applications where the fundamental frequency is 360Hz-960Hz or even higher in the future [19]. What is more, comparing with [20], sector and subsector judgement in *g-h* frame can greatly simplify calculation workload which means this identification method can avoid extra computation of β_1 and β_2 used in [20]. A similar subsector judgement method used in a novel modulation scheme, actually based on *g-h* frame concept, has been presented in [21], while the dwell time calculation still use *sin/cos* functions.

For switching sequence, according to [22], it should meet two requirements as:

a) The transition from one switching state to the next one should involve only two switches in the same converter leg, i.e. one being switched on and the other switched off.

b) The transition of V_{ref} moves from one sector in the space vector diagram to the next requires no or minimum number of switching actions.

In this paper, NP voltage balancing based on the virtual vector algorithm using *g-h* coordinate and the benefit of this method are introduced. The following paper is organized as follows: In section II, basic concepts and definitions of VSVPWM are introduced. And *g-h* coordinate will be re-defined based on virtual space vector. Sector and sub-sector judgment, dwell time calculation and other processes are specifically expressed in this new frame. Then, the optimal switching sequence will be analysed and chose properly. Finally, the relevant simulation results will be presented to demonstrate the effectiveness and correctness of this method.

II. Virtual Space Vector PWM and g-h Coordinate

A. The Definition of VSVPWM

Briefly, compared with conventional NTV-SVPWM (Nearest-Three-Vector SVPWM) drawn in Fig.2, virtual space voltage vectors are composed of a series of basic space voltage vectors which do not equivalently produce NP current during a switching cycle, thereby guaranteeing NP voltage balancing. From the definition below, it can be seen that space reference voltage, consisted by the virtual space voltage vectors that do not produce any extra NP current, can be synthesized. In that way, apparently, NP voltage problem can be significantly solved with all range of modulation index and power factor.

In order to specify these special non-neutral-point-current vectors, the basic definition can be showed as:

Define:

$$V_{Z0} = V_{0(OOO)}(0)\ V_{ZL1} = V_{L1(PNN)}(0)$$

$$V_{ZL2} = V_{L2(PPN)}(0)$$

$$V_{ZS1} = \frac{1}{2}V_{S1(POO)}(-i_a) + \frac{1}{2}V_{S1(ONN)}(i_a)$$

$$V_{ZS2} = \frac{1}{2}V_{S2(PPO)}(i_c) + \frac{1}{2}V_{S2(OON)}(-i_c)$$

$$V_{ZM1} = \frac{1}{3}V_{S1(ONN)}(i_a) + \frac{1}{3}V_{M1(PON)}(i_b) + \frac{1}{3}V_{S2(PPO)}(i_c)$$

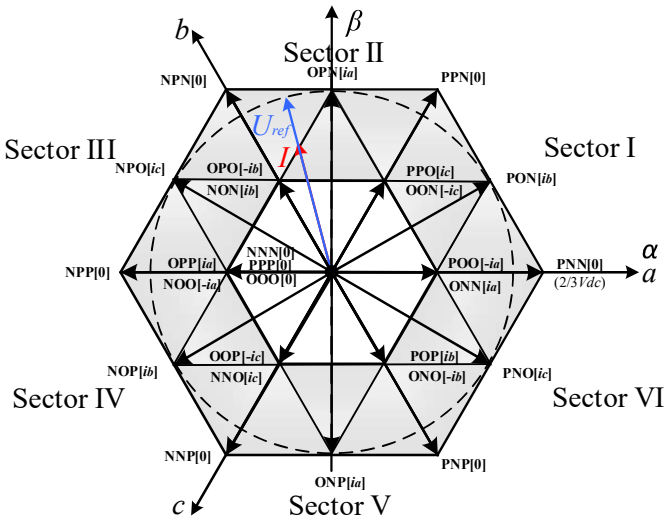

Fig. 2. The hexagon of traditional NTV-SVPWM.

B. The Definition of g-h Coordinate

The *g-h* coordinate which is also known as the 60-degree frame is transferred from orthogonal $\alpha - \beta$ frame. The transformation from the $\alpha - \beta$ frame to *g-h* can be expressed as:

$$\begin{bmatrix} V_g \\ V_h \end{bmatrix} = \begin{bmatrix} 1 & -\frac{1}{\sqrt{3}} \\ 0 & \frac{2}{\sqrt{3}} \end{bmatrix} \begin{bmatrix} V_\alpha \\ V_\beta \end{bmatrix} = \sqrt{\frac{2}{3}} \begin{bmatrix} 1 & -1 & 0 \\ 0 & 1 & -1 \end{bmatrix} \begin{bmatrix} V_a \\ V_b \\ V_c \end{bmatrix} \quad (1)$$

The virtual space vector based on *g-h* coordinate can be drawn in Fig.3. Note that the scale of space voltage vector (*g*, *h*) is nominalized with respected to the length of large vector scale. More exactly, (*1, 0*) stands for the position of vector V_{ZL1}.

According to the principle of nearest-three-vector composing, each sector can be divided into 5 parts based on NTV-VSVPWM. Sector and subsector judgment should be re-conducted in the new frame. If all the boundary lines in Fig.3 are projected into the orthogonal plane. The following diagram can be achieved. Note that both V_g and V_h are normalized with respect to the scale of V_{ZL1}, namely, $2V_{dc}/3$, which benefits programming and digital processing.

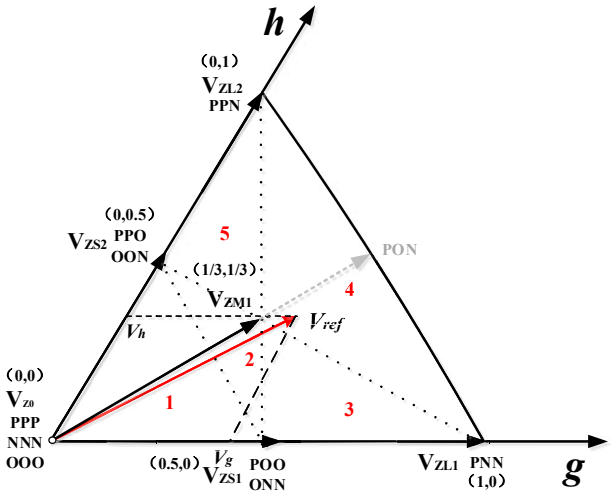

Fig. 3. Reference voltage composing using NTV-VSVPWM in sector I.

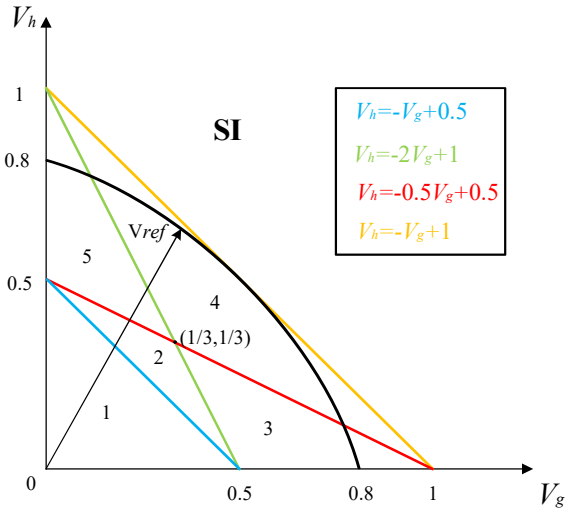

Fig. 4. Subsector detection method in sector I.

In the rebuilt *g*-*h* frame, the boundary of each subsector is listed in Table I. As can be seen, boundary lines are calculated with algebraic equations only in Fig.4. This algebraic calculation will be much easier and faster than the sinusoidal functions which are commonly used in conventional space vector modulation schemes.

The whole hexagon in *g*-*h* plane can be achieved in Fig.5.

Next, in order to conveniently judge other subsectors among sector II-VI, it should convert reference voltage into sector I. The transfer relation can be yielded as:

$$\begin{bmatrix} V_{gN} \\ V_{hN} \end{bmatrix} = \begin{bmatrix} 0 & -1 \\ 1 & 1 \end{bmatrix}^{(N-1)} \begin{bmatrix} V_{gN} \\ V_{hN} \end{bmatrix} \tag{2}$$

The relationship between V_{g1}/V_{h1} and V_{gn}/V_{hn} (n=2-6) can be listed from sector I to sector VI as follow:

According to synthesizing rules of volts-second principle based on NTV-VSVPWM, (3) can be derived as:

TABLE I
THE CRITERIA FOR SUBSECTOR JUDGMENT IN SECTOR I

Subsector	Criteria
1	$0 \le V_{g1}+V_{h1} \le 0.5$
2	$V_{g1}+V_{h1} \ge 0.5,\ V_{h1}+2V_{g1} \le 1,\ 0.5V_{g1}+V_{h1} \le 0.5$
3	$V_{h1}+2V_{g1} \ge 1,\ 0.5V_{g1}+V_{h1} \le 0.5,\ V_{h1} \ge 0$
4	$V_{g1}+V_{h1} \le 1,\ V_{h1}+V_{g1} \ge 1,\ 0.5V_{g1}+V_{h1} \ge 0.5$
5	$V_{g1} \ge 0,\ 0.5V_{g1}+V_{h1} \ge 0.5,\ V_{h1}+2V_{g1} \le 1$

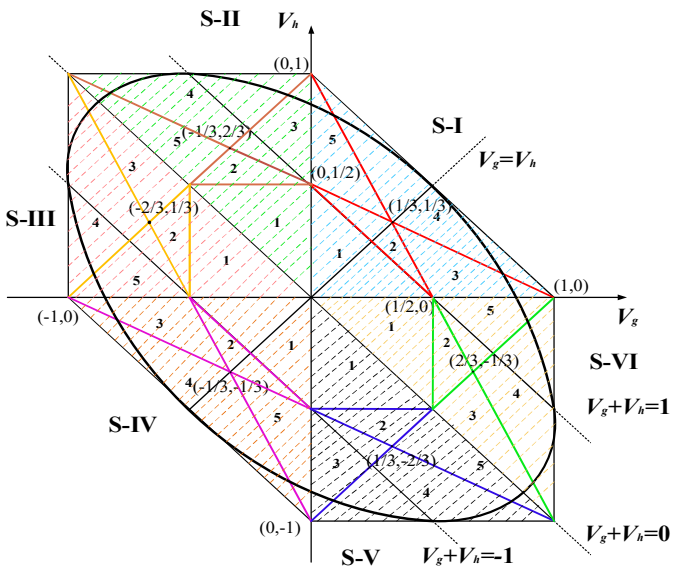

Fig. 5. Space vector diagram based on virtual space voltage vector in *g*-*h* coordinate.

$$\begin{cases} V_{ref} = V_1 d_1 + V_2 d_2 + V_3 d_3 \\ d_1 = \dfrac{T_1}{T_s}, d_2 = \dfrac{T_2}{T_s}, d_3 = V_3 \dfrac{T_3}{T_s} \\ d_1 + d_2 + d_3 = 1 \end{cases} \tag{3}$$

Using d_1, d_2 and d_3 to denote the duty cycle of dwell time among the nearest basic space vectors.

Without loss of generality, take subsector-2 for example, the nearest space vectors are V_{ZS1}, V_{ZS2} and V_{ZSM}, and the dwell time for each one are T1, T2 and T3, respectively.

TABLE II
THE FORMULA FOR SECTOR CONVERSION IN G-H COORDINATE

Sector	Formula
2	$V_{g1} = V_{h1} + V_{h2},\quad V_{h1} = V_{h2}$
3	$V_{g1} = V_{h3},\quad V_{h1} = -V_{g3} - V_{h3}$
4	$V_{h1} + 2V_{g1} \ge 1,\quad 0.5V_{g1} + V_{h1} \le 0.5,\quad V_{h1} \ge 0$
5	$V_{g1} + V_{h1} \le 1,\quad V_{h1} + V_{g1} \ge 1,\quad 0.5V_{g1} + V_{h1} \ge 0.5$
6	$V_{g1} \ge 0,\quad 0.5V_{g1} + V_{h1} \ge 0.5,\quad V_{h1} + 2V_{g1} \le 1$

$$\begin{cases} gT_s = \frac{1}{2}T_1 + \frac{1}{3}T_3 \\ hT_s = \frac{1}{2}T_2 + \frac{1}{3}T_3 \end{cases} \tag{4}$$

$$\begin{cases} g = \frac{1}{2}d_1 + \frac{1}{3}d_3 \\ h = \frac{1}{2}d_2 + \frac{1}{3}d_3 \end{cases} \tag{5}$$

Above equations, g and h are the coordinate of V_{ref} in g-h frame, 1/2 and 1/3 are the coordinates of nearby three virtual space vector, respectively. Substitute (4) and (5) into (3), the following equations can be achieved:

$$\begin{cases} d_1 = 2[1 - g - 2h] \\ d_2 = 2[1 - h - 2g] \\ d_3 = 3[2(g + h) - 1] \end{cases} \tag{6}$$

In (6), according to different subsectors, subscript 1, 2 and 3 correspond to V_{ZS1},V_{ZS2},V_{Z0}; V_{ZS1},V_{ZS2}, V_{ZM1}; V_{ZL1},V_{ZL2},V_{ZM1}; V_{ZM1}, V_{ZS1}, V_{ZL1} or V_{ZM1}, V_{ZS2}, V_{ZL2}, respectively. Similarly, in the rest of subsectors, duty cycle for each space vector can be listed as follow:

TABLE III
DIFFERENT DUTY CYCLES AMONG SUBSRCTOR 1-5

Subsector	d_1	d_2	d_3
1	$2g$	$2h$	$1-2(g+h)$
2	$2(1-g-2h)$	$2(1-g-2h)$	$3[2(g+h)-1]$
3	$2(1-2h-2g)$	$2g+h-1$	$3h$
4	$3(1-g-h)$	$2g+h-1$	$2h+g-1$
5	$2(1-2g-2h)$	$2h+g-1$	$3h$

Since there are 27 basic switching states for 3L-NPC converter, which can synthesize virtual space vectors in g-h frame, and specific dwell time for corresponding switching state should also be re-calculated. More precisely, take section I for example:

$$d_{ooo} = d_{\mathrm{VZ0}}\ d_{ppn} = d_{\mathrm{VZL2}}\ d_{poo} = \frac{1}{2}d_{\mathrm{VZS1}}\ d_{pon} = \frac{1}{3}d_{\mathrm{VZM1}}$$

$$d_{oon} = \frac{1}{2}d_{\mathrm{VZS2}}\ d_{onn} = \frac{1}{2}d_{\mathrm{VZS1}} + \frac{1}{3}d_{\mathrm{VZM1}}\ d_{ppn} = d_{\mathrm{VZL1}}$$

$$d_{ppo} = \frac{1}{2}d_{\mathrm{VZS2}} + \frac{1}{3}d_{\mathrm{VZM1}}$$

So in sector I, the dwell time is listed in Table IV.

III. OPTIMAL SWITCHING SEQUENCE BASED ON VIRTUAL SPACE VECTOR PWM

Switching sequence is an essential issue which has a great influence on AC-side voltage waveform. The virtual space vector also should use an optimized switching sequence to achieve better THD and power losses. The final selected switching sequence should satisfy the requirements in [22].

TABLE IV
THE DWELL TIME FOR DIFFERENT SWITCHING STATE IN SECTOR I

Sector Number	Dwell Time
S-I-1	d_{poo}=g d_{oon}=h d_{ooo}=1−2(g+h) d_{onn}=g d_{ppo}=h
S-I-2	d_{oon}=1−h−2g d_{onn}=g d_{poo}=1−g−2h d_{ppo}=h d_{pon}=2(g+h)−1
S-I-3	d_{poo}=1−2h−h d_{onn}=1−h−g d_{ppo}=h d_{pon}=h d_{pnn}=2g+h−1
S-I-4	d_{ppo}=1−g−h d_{ppn}=2h+g−1 d_{pon}=1−g−h d_{pnn}=2g+h−1 d_{onn}=1−g−h
S-I-5	d_{ppo}=1−g−h d_{oon}=1−2g−h d_{onn}=g d_{ppn}=2h+g−1 d_{pon}=g

In [23], authors present a symmetric switching sequence for VSVPWM, nevertheless, it uses 9-segment method to synthesize Vref. Apparently, its switching loss is a tough issue if switching frequency is relatively high. f_s in the electrical S/G system is more than three times of its counterpart in [23]. The effective switching frequency can be defined as in [24]:

$$f_{s.Eff} = \frac{f_s \times A.N.S.SPerT_s}{6} \tag{7}$$

$$P_{s.s} = f_{s.Eff} \times (E_{on} + E_{off}) \times \frac{I_s}{I_{nom}} \tag{8}$$

Where *A.N.S.S* means Average Number of Switching Steps, $P_{s.s}$ is the switching loss of IGBT, $f_{s.Eff}$ means effective switching frequency, E_{on} and E_{off} are the turn-on and turn-off energy losses, I_s and I_{nom} are actual current and nominal current, respectively, and T_s is a switching cycle.

Although it increases THD, mainly containing odds-order harmonics, in AC-side current, however, in essence higher switching frequency can significantly deal with it as a compensation. Based on this reason, switching sequence use asymmetric 5-segment method to avoid extra switching loss. To be more specific, VSVPWM with symmetric switching sequence gain 4/3 times of switching frequency while its counterpart can make it to half, and switching power loss $P_{s.s}$ can be also further decreased. Apart from that, output quality of current has more stringent requirement on even-order harmonics. More importantly, it is even-order harmonics that influence NP balancing problem to some extent. Therefore, it should be eliminated from the modulation perspective, and then optimal switching sequence should be chose properly.

Namely, line-to-line voltage need to meet the condition of $V_{AB}(\omega t)=-V_{AB}(\omega t+\pi)$. Such as S-I-1 and S-IV-1, switching states can be chose according to the following sequence in Table.V. And also, from Fig.6 (b), it can obviously satisfy the requirement of even-order harmonics reduction, that is $V_{AB}(\omega t)=-V_{AB}(\omega t+\pi)$.

IV. Simulation Results

To validate the developed modulation scheme for the three-level NPC converter, a behavioral model was established and simulated in a Matlab/Simulink and PLECS environment. The simulated system is shown in Fig.7 with system parameters listed in Table VI.

In Starter/Generator system of MEA, PMSM always run as a high-speed drive, in order to sufficiently use DC-bus voltage, the approximate modulation index is 0.98. Hence, the subsectors that the tip of V_{ref} wipes are 3/4/5. Sector and subsector judgment waveforms are well detected in Fig.8.

From Fig.9, it can be seen that d_x(*x*=VT_{i1}, VT_{i2}, VT_{i3}, VT_{i4} and *i*=*A*-, *B*-, *C*- phase) is the duty cycle function of each IGBTs in each arms. Duty cycle function of VSVPWM also looks like saddle because of third harmonics injection comparing with SPWM.

In Fig.10 (a), the phase-A current waveform can be showed and phase currents THD is approximately 4.3%. In Fig.10 (b), the FFT analysis shows there is no harmonics at even-order frequency, which can demonstrate the functionality of this switching sequence.

TABLE V
Optimal Switching Sequence Based on Virtual Space Vector PWM

Sector/Subsector Number	Switching Sequence
S-I-1	ONN OON OOO POO PPO
S-I-2	PPO POO PON OON ONN
S-I-3	ONN PNN PON POO PPO
S-I-4	PPO PPN PON PNN ONN
S-I-5	ONN OON PON PPN PPO
S-II-1	PPO OPO OOO OON NON
S-II-2	NON OON OPN OPO PPO
S-II-3	PPO PPN OPN OON NON
S-II-4	NON NPN OPN PPN PPO
S-II-5	PPO OPO OPN NPN NON
S-III-1	NON NOO OOO OPO OPP
S-III-2	OPP OPO NPO NOO NON
S-III-3	NON NPN NPO OPO OPP
S-III-4	OPP NPP NPO NPN NON
S-III-5	NON NOO NPO NPP OPP
S-IV-1	OPP OOP OOO NOO NNO
S-IV-2	NNO NOO NOP OOP OPP
S-IV-3	OPP NPP NOP NOO NNO
S-IV-4	NNO NNP NOP NPP OPP
S-IV-5	OPP OOP NOP NNP NNO
S-V-1	NNO ONO OOO OOP POP
S-V-2	POP OOP ONP ONO NNO
S-V-3	NNO NNP ONP OOP POP
S-V-4	POP PNP ONP NNP NNO
S-V-5	NNO ONO ONP PNP POP
S-VI-1	POP POO OOO ONO ONN
S-VI-2	ONN ONO PNO POO POP
S-VI-3	POP PNP PNO ONO ONN
S-VI-4	ONN PNN PNO PNP POP
S-VI-5	POP POO PNO PNN ONN

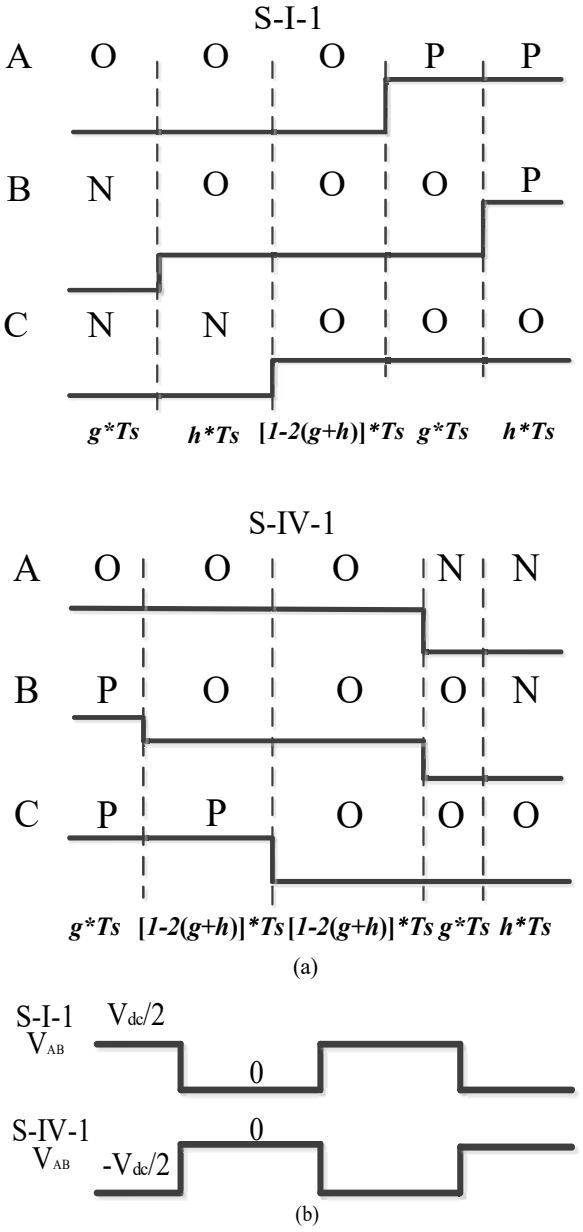

Fig. 6. (a) PWM signals in S-I-1and S-IV-1 (b) The comparison waveform of V_{AB} in S-I-1 and S-IV-1.

TABLE VI
System Parameters

Simulation Parameter	Value
PMSG output phase-voltage	115V
AC-side frequency	400Hz
Switching frequency	16kHz
DC-bus voltage	270V
Load	120Ω
Capacitor(C1=C2)	9×10^{-6}F
Inductance(L)	1.35×10^{-3}H

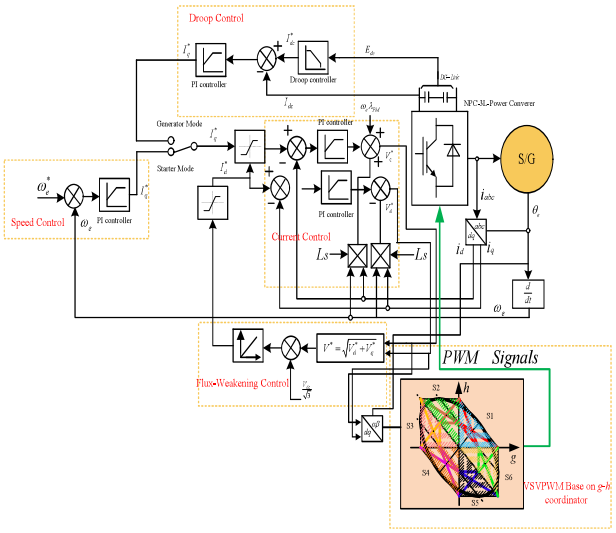

Fig. 7. The simulated S/G electrical power system.

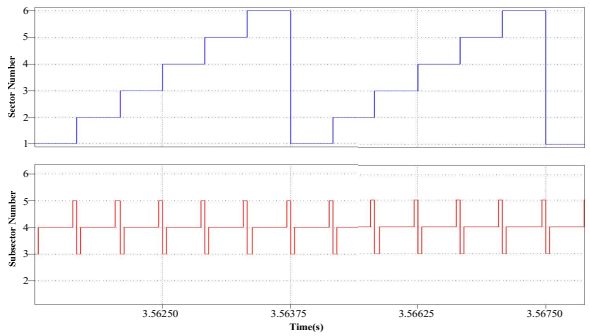

Fig. 8. Sector and subsector judgment waveform.

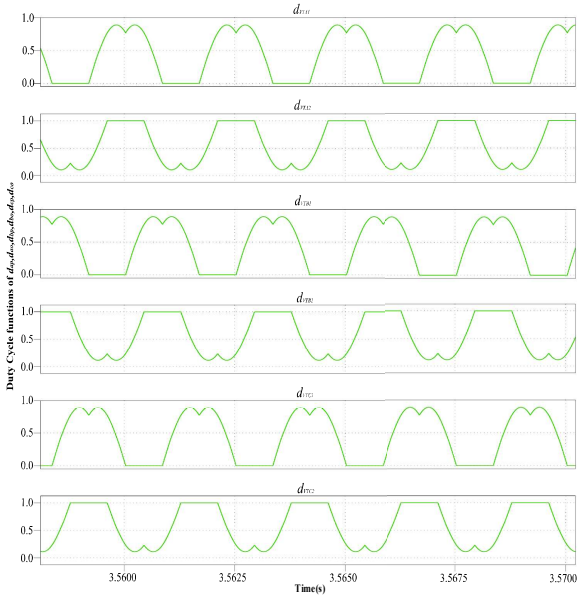

Fig. 9. Duty cycle functions waveform of d_{ap}, d_{ao}, d_{bp}, d_{bo}, d_{cp}, d_{co}.

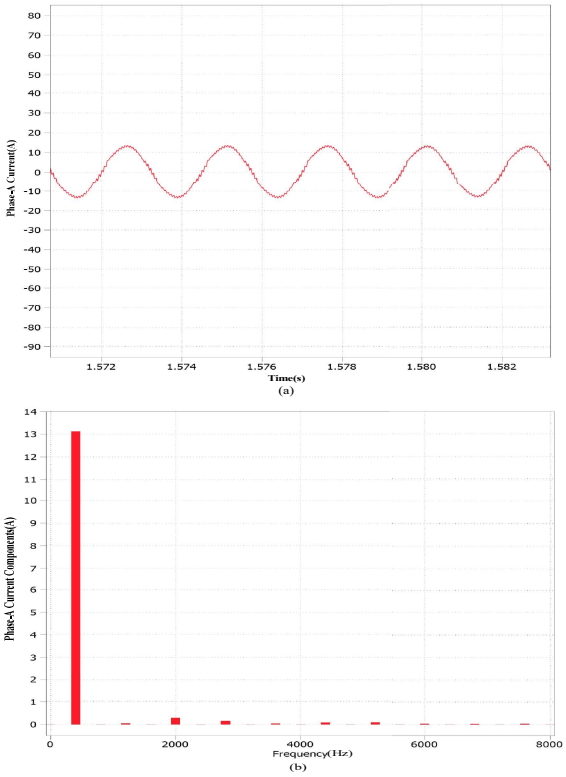

Fig. 10. (a) Phase-A current waveform with VSVPWM. (b) Fourier analysis of phase-A current.

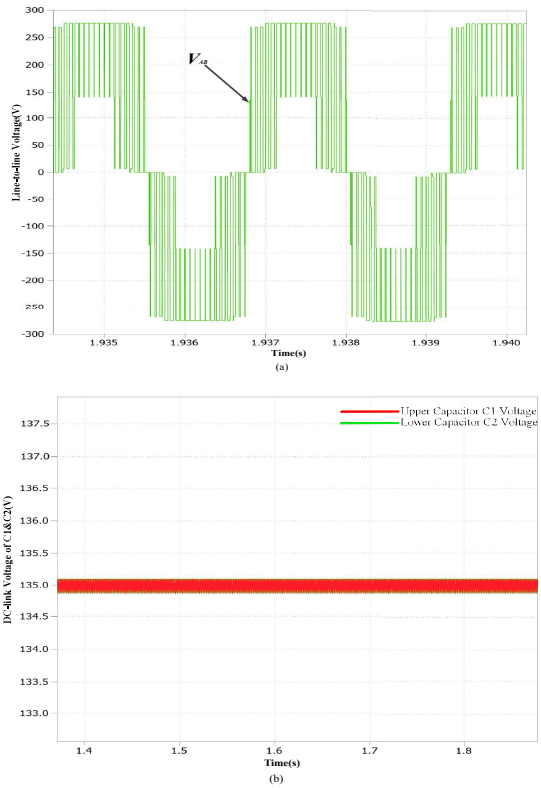

Fig. 11. (a) Line-to-line voltage of pole voltage between phase A and B. (b) Upper and lower capacitor voltage waveform.

Line-to-line voltage between phase-A and -B can be showed in Fig.11(a), it can be apparently seen that there is the overlapping regions in V_{AB} [25]. This phenomenon is different from conventional SVPWM. The DC-bus voltage between C_1 and C_2 can be dynamically depicted in Fig.11(b). From the waveform, it can be seen that VSVPWM does not bring any NP voltage unbalancing issue between upper and lower capacitors. Therefore, it can greatly solve the NP voltage drift in 3L-NPC power converter. Accordingly, it gains benefits based on VSVPWM at the expense of a bit low-odds-order distortion in the AC-side.

V. Conclusion

Virtual space vector PWM based on *g-h* coordinate and its switching sequence are proposed in this paper. Because this method substantially uses virtual space vectors that all have special coordinates in 60-degree frame, comparing with traditional $\alpha-\beta$ coordinate used in VSVPWM, it can easily express the boundary condition of sector/subsector and corresponding dwell time function in simple algebraic expression. It is obvious that not only can it avoid using *sin/cos* functions which mainly is a computational burden, but also it is convenient to program and debug by using C-code. Additionally, in order to eliminate even-order harmonics in phase current, the paper presents an optimal switching sequence. Simulation results can verify the effectiveness and correctness of this method.

Acknowledgment

The research has been supported by Clean Sky 2 (Systems ITD, project EMINEO), European H2020 program. The author F. Guo would like to thank China Scholarship Council (CSC) for sponsoring part of his Ph.D studentship.

References

[1] A. Nabae, I. Takahashi, H. Akagi, A New Neutral-Point-Clamped PWM Inverter,, IEEE Transactions on Industry Application, Vol. 1A-17, No. 5, 1981, pp. 518-523.

[2] A. Griffo, D. Drury, T. Sawata, and P. H. Mellor, Sensorless starting of a wound-field synchronous starter/generator for aerospace applications, IEEE Transactions on Industrial Electronics, Vol. 59, 2012, pp. 3579-3587.

[3] B. S. Bhangu and K. Rajashekara, Control strategy for electric starter generators embedded in gas turbine engine for aerospace applications, Energy Conversion Congress and Exposition (ECCE), 2011, pp. 1461-1467.

[4] B. S. Bhangu and K. Rajashekara, Control strategy for electric starter generators embedded in gas turbine engine for aerospace applications, Energy Conversion Congress and Exposition (ECCE), 2011, pp. 1461-1467.

[5] R. H. Williams, M. P. Foster, D. A. Stone, and S. R. Minshull, Utilizing existing aircraft wound field generators for starter-generators, IEEE 8th International Conference on Power Electronics and ECCE Asia (ICPE & ECCE), 2011, pp. 691-696.

[6] G. Calzo, P. Zanchetta, C. Gerada, A.Gaeta, F. Crescimbini, Converter topologies comparison for more electric aircrafts high speed Starter/Generator application, IEEE Energy Conversion Congress and Exposition (ECCE), 2015, pp. 3659-3666.

[7] R. Rojas, T. Ohnishi, et al., An Improved Voltage Vector Control Method for Neutral-Point-clamped Inverters, IEEE Transactions on Power Electronics, Vol. 10, No. 6, pp.666672, 1995.

[8] D. Zhou, A Self-Balancing Space Vector Switching Modulator for Three-Level Motor Drives, IEEE Power Electronics Specialist Conference (PESC), 2001, pp. 1369-1374.

[9] J. Pou, D. Boroyevich, and R. Pindado, New feedforward space-vector PWM method to obtain balanced ac output voltages in a three-level neutral-point-clamped converter, IEEE Transactions on Power Electronics, Vol. 49, Oct. 2002, pp. 1026-1034.

[10] Y. Jiao, F. Lee, S. Lu, Space Vector Modulation for Three-Level NPC Converter With Neutral Point Voltage Balance and Switching Loss Reduction, IEEE Transactions on Power Electronics, Vol. 29, No.10, Oct., pp. 5579-5591.

[11] A. Lewicki, Z. Krzeminski, H. A. Rub, Space-Vector Pulse width Modulation for Three-Level NPC Converter With the Neutral Point Voltage Control, IEEE Transactions on Industrial Electronics, Vol.58, No.11, Nov., 2011, pp. 5076-5086.

[12] C. Xiang, C. Shu, D. Han, B. Mao, X. Wu, T. Yu, Improved Virtual Space Vector Modulation for Three-Level Neutral-Point-Clamped Converter With Feedback of Neutral-Point Voltage, IEEE Transactions on Power Electronics, Vol. 33, No, 6, June, 2018, pp. 5452-5464.

[13] S. Monge, J. Bordonau, D. Boroyevich, S. Somavilla, The Nearest Three Virtual Space Vector PWMA Modulation for the Comprehensive Neutral-Point Balancing in the Three-Level NPC Inverter, IEEE Power Electronics Letters, Vol.2, No.1, Mar, 2004, pp. 11-15.

[14] G. Narayanan, D. Zhao, H. K. Krishnamurthy, R. Ayyanar and V. T. Ranganathan, "Space Vector Based Hybrid PWM Techniques for Reduced Current Ripple," in IEEE Transactions on Industrial Electronics, Vol. 55, No. 4, April, 2008, pp. 1614-1627.

[15] Z. Huang, T. Yang, P. Giangrande, P. Wheeler and M. Galea, "An effective hybrid space vector PWM technique to improved inverter performance," 2017 IEEE Southern Power Electronics Conference (SPEC), Puerto Varas, 2017, pp. 1-6.

[16] F. Wang, "Reduce Beat and Harmonics in Grid-Connected Three-Level Voltage-Source Converters With Low Switching Frequencies," IEEE Transactions on Industry Applications, Vol. 43, No. 5, Sep.-Oct. 2007, pp. 1349-1359.

[17] C. Liu, B. Wu, D. Xu, N. Zargari and S. Rizzo, "Progressive natural balance of neutral-point voltage of three-level NPC inverter with a modified SVM scheme," Twenty-First Annual IEEE Applied Power Electronics Conference and Exposition, 2006. APEC '06., Dallas, TX, 2006, pp. 4 pp. 1666.-1669.

[18] Dengming Peng, F. C. Lee, D. Boroyevich, A novel SVM algorithm for multilevel three-phase converters, 2002 IEEE 33rd Annual IEEE Power Electronics Specialists Conference. Proceedings, Vol.2, 2002, pp. 509-513.

[19] V. Madonna, P. Giangrande and M. Galea, "Electrical Power Generation in Aircraft: review, challenges and opportunities," IEEE Transactions on Transportation Electrification, 2018, pp.1-1. (Early Access)

[20] A. Choudhury, P. Pillay, S. S. Williamson, DC-Bus Voltage Balancing Algorithm for Inverter Drive With Modified Virtual Space vector, IEEE Transactions on Industrial Application, Vol.52, No.5, Sep./Oct., 2016, pp. 3958-3967.

[21] C. Li, T. Yang, et al, A Modified Neutral-Point Balancing Space Vector Modulation for Three-Level Neutral Point Clamped Converters in High Speed Drives, IEEE Transactions on Industrial Electronics, 2018, pp. 1-1. (Early Access)

[22] B. Wu. High-Power Converter and AC-Drives, IEEE Press, 2006.

[23] C. Q, Xiang, C. Shu, D. Han, B.K, et al. Improved Virtual Space Vector Modulation for Three-level Neutral-Point-Clamped Converter with Feedback of Neutral-point Voltage, IEEE Transactions on Industrial Electronics, Vol.33, No.6, June, 2018, pp. 5452-5464.

[24] G. I. Orfanoudakis, M. A. Yuratich and S. M. Sharkh, "Nearest-Vector Modulation Strategies With Minimum Amplitude of Low-Frequency Neutral-Point Voltage Oscillations for the Neutral-Point-Clamped Converter," IEEE Transactions on Power Electronics, vol. 28, no. 10, Oct. 2013, pp. 4485-4499.

[25] C. Xiang, H. Shao, Y. Zhang, X. He. Adjustable proportional hybrid SVPWM strategy for neutral-point-clamped three-level inverters, IEEE Transactions on Industrial ElectronicsVol.60, No.10, Oct, 2013, pp. 4234-4242.